POLITECNICO DI TORINO
Repository ISTITUZIONALE

A deployable and Retractable Inflatable Link for a Space Robotic Manipulator

(Article begins on next page)

03 February 2025

IAC-24,C2,IPB,13,x83275

A deployable and Retractable Inflatable Link for a Space Robotic Manipulator

**Pierpaolo Palmieri*, Matteo Gaidano, Matteo Melchiorre, Laura Salamina,
Davide Sorli, Mario Troise and Stefano Mauro**

Politecnico di Torino, Department of Mechanical and Aerospace Engineering
pierpaolo.palmieri@polito.it, matteo.gaidano@polito.it, matteo.melchiorre@polito.it, laura.salamina@polito.it,
davide.sorli@polito.it, mario.troise@polito.it, stefano.mauro@polito.it.
* Corresponding Author

Abstract

This paper presents the development of IDRA, an Inflatable and Deployable Robotic Arm for space applications. IDRA allows significant volume savings, a critical factor in space missions, and offers a workspace expansion beyond the capabilities of conventional space robotic manipulators. Moreover, its compact nature during launch offers efficient cargo space utilization, which can lead to reduced launch costs. The robot has a hybrid structure made of inflatable links and rigid electric-actuated joints. Therefore, when links are deployed, the robot has the same mode of operation of a traditional one, controlled through standard visual servoing algorithms. The ability to deploy and retract allows to occupy volume only when needed, reducing the exposure to space debris impacts and extreme conditions.

IDRA can be employed in satellites with high economic value for inspection, maintenance and servicing activities to extend their operational life, contributing to the mitigation of space debris issue. In-orbit servicing, assembly and manufacturing (ISAM) is a growing trend in the space industry and new innovative, economic and sustainable systems are required to improve the sustainability of the sector. The robotic system could be deployed only when necessary and, when stored, would have little impact on the overall volume of the satellites.

This paper focuses on the advancements in the design, analysis and verification of the inflatable link of IDRA, the key component that enables the efficient deployment and retraction of the robot. The link is designed to maintain structural integrity and operational precision of the robotic manipulator when inflated, conserving a cylindrical shape. A test bench has been constructed to test a planar version of the robotic system under simulated microgravity conditions, utilizing air bearings on an epoxy resin floor to minimize friction. The inflatable link is tested to validate its controllability and stability during the retraction phase. Results confirmed the functionality of the inflatable link mechanism, highlighting areas for potential refinement in future iterations to further enhance performance. Next steps regard the test of the inflatable links under extreme conditions, such as high and low temperature and vacuum.

Keywords: space robotics; deployable structures; robotic manipulator; inflatable structures.

1. Introduction

The term On-Orbit Servicing (OOS) refers to the maintenance of space systems in orbit, including assembly of large structures, repair, refuelling and upgrade using external satellites [1]. The broader concept of In-Space Servicing, Assembly, and Manufacturing (ISAM) encompasses OOS, including in-situ manufacturing of components, as demonstrated in the OSAM-2 project, where 3D-printed structural beams were tested [2]. In the past, OOS in low Earth orbit (LEO) primarily depended on astronauts performing extravehicular activities (EVAs). However, the harsh conditions of space, such as vacuum, microgravity, intense radiation, and extreme temperature variations, present considerable operational difficulties and dangers to human safety. To address these challenges, space robotics has become a crucial alternative, providing dependable and robust solutions that significantly improve the safety and efficiency of on-orbit operations, thereby reducing the risks to human life [3].

The ISAM market is emerging as one of the most promising and innovative areas in the space exploration landscape. The increasing complexity of space missions and the need to maintain and enhance the performance of in-orbit assets are the main growth drivers of this market. Northern Sky Research (NSR) and SpaceTec Partners have developed separate analyses to evaluate the overall market size. In 2019, NSR projected a total of $4.5 billion in ISAM revenues by 2028 [4]. Today, most satellites launched into orbit have limited maintenance capabilities. Companies operating in the ISAM market therefore aim to improve the operational efficiency and lifespan of satellites by providing in-orbit repairs, upgrades, and payload exchanges. The report produced by ESPI in 2020 highlights the exponential trend of critical and non-critical failures that will affect satellites in orbit until 2030 [5]. According to NSR, the increasing focus on space debris and the success of the commercial Mission Extension Vehicle 1 (MEV-1) create positive conditions for future commercial opportunities [6]. The

ISAM market value reached approximately $2.21 billion in 2022 [7] and $2.40 billion in 2023 [8], confirming the growth projected by NSR. Moreover, until 2028 the market could reach a value of over €5 billion, with a compound annual growth rate (CAGR) of 11%.

Suitable space robotics technologies can be used in ISAM applications, where their use has been proved in manned and unmanned missions [9]. In the past, launcher failure was the most common cause of mission failure. However, today the on-orbit failures have exceeded launch failures [10]. Technological advancements in launch systems have resulted in the successful deployment of over 4,300 satellites, predominantly in LEO [11], contributing to the complexity and density of space assets. This expansion has led to a parallel rise in orbital debris, with current estimates identifying approximately 2,000 objects larger than 1 cm orbiting Earth, necessitating advanced monitoring and collision mitigation strategies [12], Prepare for impact: Space debris and statistics]. Moreover, every launched satellite eventually runs out of fuel and thus, must be decommissioned.

ISAM activities aimed at extending the lifespan of satellites will be carried out using robotic manipulators [13], with several projects aimed at reducing space debris accumulation [14, 15]. The need to efficiently repair, assist, and maintain geostationary satellites is driving the market growth for manipulators in space applications. The global space robotics market reached a $4.3 billion value in 2021. By 2031, the market will reach $8 billion, with a CAGR of 6.9%. The space manipulators market currently represents 25% of the space robotics market, with an overall growth of 300% over 10 years [16]. Northrop Grumman's Mission Extension Vehicle (MEV), developed through its Space Logistics subsidiary, represents a significant advancement in ISAM. A key milestone was achieved in 2022 when the MEV-2 successfully docked with the Intelsat 10-02 satellite, extending its operational life by five years through refuelling [17]. However, the high costs associated with using an additional spacecraft equipped with a manipulator make this approach convenient only for high-value assets, typically located in geosynchronous orbit (GEO) [18].

In the last decades, space research has focused on the development of deployable structures to enhance payload-to-weight ratios. This approach aims to balance the demands of large-scale aerospace projects with the restricted payload capacity of launch vehicles. Research on inflatable booms in space environments [19] has shown that inflatable structures are both feasible and reliable. Inflatable structures offer great potential due to their low mass and ability to be rapidly reshaped, inflated, and solidified into desired modular units, which can then be assembled into large, complex configurations. Furthermore, inflatable technology allows for overcoming the limitations of other solutions, such as additive construction and assembly methods, which it has the major challenge of still having to transport large and heavy robotic equipment required to perform complex construction. The deployment strategy od inflatable space system can be implemented through various methods [19]. For instance, inflatable booms can be deployed in stages, inflating one compartment at a time until the structure achieves the required pressure and rigidity. This method provides greater stability compared to free-inflation techniques [20]. Different architectures have been proposed for inflatable manipulators, some combining inflatable links with rigid joints and electric actuation [21], while others employ fully soft structures with pneumatic actuation [22]. However, the performance of such systems must be evaluated using flexible body models [23]. A pioneering project in this domain was the Inflatable Antenna Experiment (IAE) [24] in 1996. More recently, inflatable habitats have garnered interest, particularly for next-generation space stations and lunar habitats, as exemplified by the Bigelow Expandable Activity Module (BEAM) deployed on the ISS in 2016 [25]. Sierra Space is continuing advancements in this field with their LIFE module [26]. Inflatable manipulators offer several advantages for space applications, particularly in ISAM missions, where volume savings are critical. These technologies could also prove valuable for operations on lunar and Martian terrains, where their adaptability and reduced logistical footprint could significantly enhance mission success and viability.

Space robotic manipulators have been primarily used on the International Space Station (ISS) in the past to support astronauts' extravehicular activities, including the Canadian Mobile Servicing System (MSS), the Japanese Experiment Module Remote Manipulator System (JEMRMS), and the European Robotic Arm (ERA) [27]. Furthermore, several onboard robotic systems have been proposed to assist astronauts in daily activities [28, 29], with ongoing research exploring the potential use of inflatable manipulators onboard spacecraft [30]. Soft robots with contact-detection algorithms [31] can improve safety by absorbing energy during accidental impacts. Moreover, inflatable manipulators can be tailored for human-robot collaboration (HRC) [32], with vision-based state estimation and collision-avoidance algorithms [33-36] ensuring safe interactions in shared workspaces.

This paper introduces the Inflatable and Deployable Robotic Arm (IDRA), a robotic system designed for OOS, with a focus on the development of its inflatable links. The robotic manipulator can achieve a large operational workspace due to its inflatable design, which enables a high packing ratio and efficient deployment. After outlining the conceptual framework, the work presents the progression from early prototypes [37] to the

current iteration of the link, which incorporates mechanisms for controlled deployment and retraction, maintaining the link's cylindrical shape and stability throughout the process. A dedicated test rig has been constructed to test a planar version of IDRA under simulated microgravity conditions. A prototype of inflatable link is testes to validate the automatic retraction, highlighting the system's feasibility and laying the groundwork for future advancements in the complete robotic system. The next steps involve further refinement and testing to optimize the system's performance, followed by the assembly of the full prototype for microgravity testing.

2. IDRA's Concept and Mission

The IDRA is a robotic system engineered for space applications, featuring a hybrid design that combines inflatable links with rigid, electrically actuated joints. This approach leverages the benefits of deployable structures to minimize the system's volume when stowed, which is advantageous for space missions, while the electric joints ensure stable and precise movement using standard control techniques.

The inflatable links are designed with multiple internal chambers within each segment, enhancing stability and control during deployment and retraction phases and introducing modularity that can easily adapt the system to different workspace. In Fig. 1, a rendering of IDRA mounted on a satellite is presented, depicting the deployment phase of the second link. The robotic manipulator features 7 degrees of freedom (DOFs) and incorporates two inflatable links. However, alternative configurations with 6 DOFs or additional inflatable links may be explored for specialized applications where enhanced system dexterity is required.
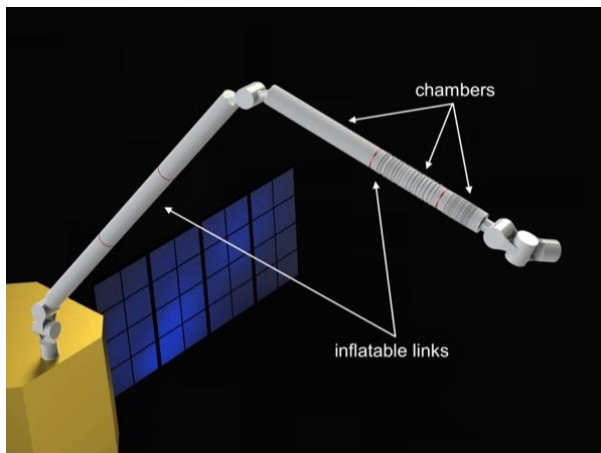

Fig. 1. IDRA mounted on a satellite. Inflatable links and chambers.

IDRA operates at relatively low pressures, ranging from 10 kPa to 100 kPa, to achieve great payload capacities and structural integrity, as discussed in the subsequent sections.

Due to the high packing ratio achievable with inflatable links, the robotic system can reach a larger operational workspace compared to traditional technologies, given the same stowed volume. Assuming a packing ratio of 4:1, consistent with preliminary technology development, IDRA can extend its workspace beyond the dimensions of most satellites.

Consequently, IDRA has the potential to enable self-maintenance capabilities when integrated into next-generation satellites. The robotic system can function as a safety mechanism designed to extend the operational lifespan of high-value, medium-to-heavy class satellites, such as the COSMO-SkyMed satellites. [38]. Thanks to its large workspace, IDRA can access any part of the satellite and perform a wide range of servicing tasks. The range of tasks the robot can perform is contingent upon the tools available at its end-effector. Therefore, an analysis is necessary to identify and design a toolkit to be mounted on the satellite, comprising various tools tailored for different operations. The primary tasks include detailed close-range inspections and repair activities, such as supporting the recovery of failed deployments of antennas or solar arrays. In future applications, the robotic system could also facilitate upgrading operations, such as berthing augmentation modules to the satellite. For instance, refuelling pods could be installed to extend the satellite's operational lifespan.

The robotic system has a broad range of potential alternative applications. It can be integrated onto a servicing satellite to conduct on-orbit servicing (OOS) operations and actively remove space debris, as proposed in previous studies [39, 40]. It can be utilized on space stations for onboard operations to assist astronauts. The system can be stowed when not in use and deployed as needed for specific experiments, as proposed in [30]. Potential applications on the Moon and Mars include integration with rovers and drones. More broadly, the system is well-suited for scenarios where minimizing volume is a critical requirement.

3. Inflatable Links
Inflatable links are a relevant component in the design and functionality of inflatable robots. These links enable the robot to handle significant payloads while ensuring an effective deployment and retraction. This involves selecting the right materials, optimizing the link structure, and integrating a reliable pneumatic system.

3.1 Collapse Load
The inflatable links of the robot can be modelled as beams since the pre-stress due to the pressure supply stiffens the structure. When a beam is bent, structural failure occurs when the applied moment reaches the

collapse moment M_c. For preliminary design purposes, membrane-based formulations are effective for estimating the dimensions of the inflatable link in relation to its load-bearing capacity. The equation for M_c as proposed by Wielgosz et al. [41], is presented below:

$$M_c = \frac{\pi^2}{4} pr^3 \qquad (1)$$

where p is the relative pressure, and r is the radius of the link. Let's consider as critical condition the wrinkling moment M_w that is assumed in literature as half the collapse moment M_c [42]. Considering the external transverse force F_y, which is the inertial force generated by the motion of the payload, the link's length L, the internal pressure must satisfy the following condition:

$$p \geq \frac{2F_y L}{\pi r} \qquad (2)$$

After an initial iteration using simplified formulations, more advanced models can be employed for a refined analysis. In NASA SP 8007 (1968) [43], the collapse moment is calculated using semi-empirical methodology, which combines three components: the moment-carrying capacity of a pressurized membrane cylinder reduced to 80% of the theoretical value for design purposes, the collapse moment of an unpressurized cylinder considering material thickness and tensile modulus, and an enhancement in the critical moment resulting from pressurization.

3.2 Pneumatic line

The tank's bulk, needed for inflation, is small to the robot's dimensions, allowing it to store pressurized fluids in liquid form, such as R134a, commonly used in small satellites. The overall pneumatic system is simple, comprising a pressurized tank, a pressure-reducing valve that menages the desired pressure for the chambers, and digital valves that controls the inflation and deflation phases for each chamber.

3.3 Layers and Materials

The structural design of IDRA must incorporate considerations analogous to those used in the TransHab [44, 45], LIFE module [26], and various studies on inflatable lunar habitats [46]. This involves a focus on three key layers: the bladder, the restraint, and the protection layers. The design specifications for IDRA can be less stringent than those for human-habitable modules, allowing for potential adjustments in material selection and layer thickness.

The restraint layer, or structural layer, is crucial as it bears the loads from inflation. It must be designed to handle both hoop and axial stresses, requiring materials with high tensile strength. This layer should also be foldable and deployable, maintaining structural integrity during deployment and operation in orbital conditions. Materials such as Kevlar, used in the BEAM experiment, and Vectran, employed in Sierra Space's LIFE module, are suitable for this purpose. Table 1 presents a comparison of Zylon HM, Kevlar 49, and Vectran UM, highlighting their tensile modulus and density relative to aluminum. These materials exhibit superior tensile modulus and lower density compared to aluminum, with near-zero coefficients of thermal expansion (CTE), high resistance to temperature extremes, abrasion, creep, and radiation, as well as effective vibration damping and impact strength for debris shielding [47, 48].

The bladder layer is responsible for maintaining internal pressure and thus must possess flexibility, durability, and low permeability over a wide temperature range. An alternative approach to separate bladder and restraint layers is the use of coated textiles, which combine structural rigidity and tensile strength with effective pneumatic hermeticity. Coatings also protect the underlying fibers from environmental and mechanical degradation.

Table 1. Restrain layer candidate materials

Material	Tensile Modulus (GPa)	Density (g/cm^3)
Zylon HM	270	1.56
Kevlar 49	112	1.44
Vectran UM	103	1.40

3.1 Mechanism for deployment and retraction

The deployment and retraction mechanism enables the gradual inflation and deflation of the link chambers. The mechanism is designed to control the deployment and retraction process gradually, maintaining the cylindrical shape and allowing movement along the link axis. Fig. 2 illustrates this mechanism with three chambers for clarity.
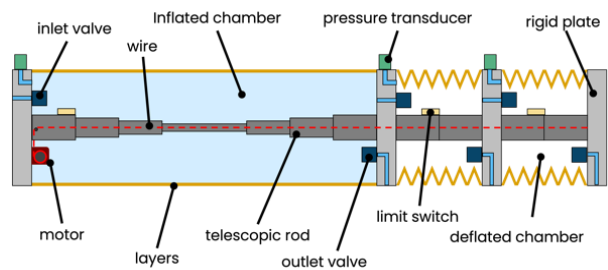

Fig. 4. Mechanism for controlled deployment and retraction of the inflatable link with 3 chambers.

Each chamber is equipped with two digital valves: one for inflation and one for deflation. The valves are normally closed to ensure energy savings, as they are active only during the deployment or deflation phase. Inside each chamber, a telescopic rod runs along its axis,

helping to maintain the cylindrical shape and prevent twisting during inflation and deflation. The rod achieves a packing ratio of 4:1, meaning it can compress to a quarter of its full size. A wire runs inside this rod, passing through rigid plates that separate the chambers. This wire connects the last plate to an electric motor located in the first chamber. The motor retracts the link by pulling the wire while the outlet valves are activated. Pressure transducers are installed to monitor the pressure in each chamber. Initially, with the inlet valve closed, the chamber is deflated, marking Phase 0. When the inlet valve opens, gas flows into the chamber, initiating its expansion in Phase 1. During this phase, the motor remains inactive, while the telescopic rod guides the expansion along the link's axis. Once the chamber reaches its full size and the desired pressure, the inlet valve closes, concluding Phase 2. This sequence is then repeated in the second chamber to fully inflate the link. For retraction, the outlet valve opens, releasing the gas. Simultaneously, the motor activates, retracting the rigid plate and compressing the chamber to speed up the gas outflow. The telescopic rod again assists by guiding the retraction

4. Design and Prototypes

Theoretical design methodologies, integrated with dynamic multibody models [reference-tesi PP], facilitate the development of preliminary prototypes to validate the concept, enabling the definition of link dimensions based on the desired performance criteria.

A preliminary prototype, shown in Fig. 3, was constructed using polymeric materials that function as the bladder and restraining layers, enabling functional verification of the robotic system. Static and dynamic testing of the links validated the theoretical design criteria, confirming both payload capacity and structural stiffness [37]. The prototype, consisting of three electric motors, with links measuring 600 mm in length, radius of 85 mm and 55 mm for each link, demonstrated effective controllability with a payload capacity of 2 kg in a laboratory setting.
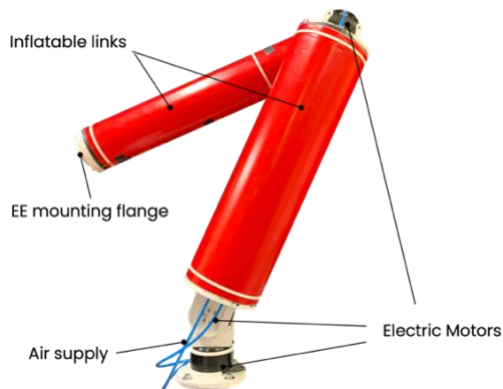

Fig. 3. Preliminary prototype with polymeric materials.

This prototype did not incorporate the mechanism for controlled deployment and retraction. Additionally, the links lacked a pattern necessary to ensure controllability during these phases. It is crucial to maintain full control over the system while preserving the cylindrical shape of the links during deployment and retraction, ensuring structural integrity in the fully deployed state and optimal compactness when stowed. The mechanism for controlled deployment and retraction must be integrated with layers featuring a specific folding pattern to facilitate these operations. During the retraction phase, the folding pattern should exhibit sufficient stiffness to generate wrinkles at predefined locations, enabling precise contraction. For the deployment phase, the choice of pattern is less critical, as various packing techniques are documented in the literature [49], including wrapping [50], Z-fold, and more intricate origami-inspired designs. The primary challenges involve achieving precise, controlled, and predictable deployment while ensuring post-deployment stability of the articulated links.

In this study, a pattern employing rigid elliptical elements interconnected via hinges is utilized [51]. This configuration has demonstrated superior reversibility and performance during both deployment and retraction phases. The principle is illustrated in Fig. 4. The ellipses are designed with a pitch that prevents the outer layer from contacting the inner telescopic rod of the mechanism, ensuring unobstructed movement and minimizing mechanical interference.
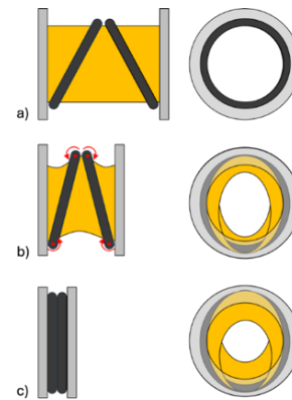

Fig. 4. Folding pattern principle.

A prototype of the chamber, depicted in Fig. 5, was constructed to evaluate its functional performance. The prototype features a bladder layer made of polyurethane (PU) and a restraining layer composed of Kevlar. This configuration was designed to test various parameters, including structural integrity, gas impermeability, stability of the cylindrical geometry, packing efficiency, as well as deployment and retraction capabilities. The folding pattern has been embedded within the bladder layer to enhance the controlled deformation and mechanical response during operational cycles.
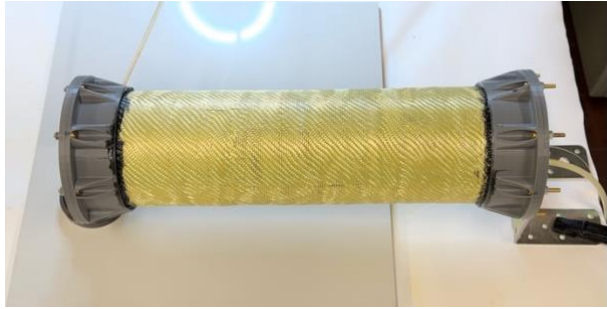
Fig. 5. Prototype of link chamber with pattern structure, bladder layer in PU and restrain layer in Kevlar.

A preliminary prototype of the deployment and retraction mechanism, shown in Fig. 6, has been assembled to conduct functional tests focused on the mechanical system and control algorithms. The prototype includes a telescopic rod equipped with cable management supports for optimal organization during the compacted phase of the chamber.
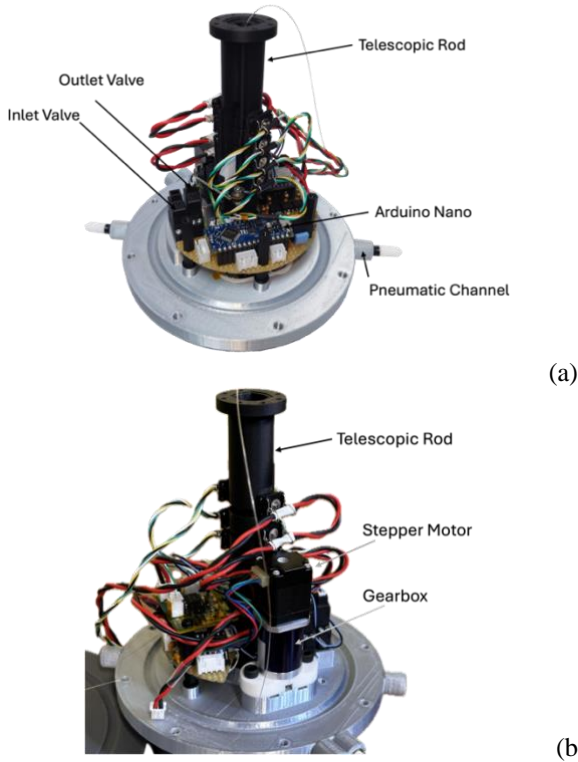

(a)

(b)

Fig. 6. Functional prototype of the mechanism for controlled deployment and retraction.

It features inlet and outlet valves integrated with channels on the plate to facilitate inflation and deflation operations. A NEMA 8 stepper motor, paired with a 90:1 gearbox, delivers the retraction forces necessary for the mechanism by pulling a nylon wire anchored to the opposite plate. The motor is controlled by an Arduino Nano. All mechanical components have been fabricated

using additive manufacturing with PLA, while the telescopic rod was made from carbon fiber-reinforced PLA to provide enhanced mechanical strength. Pressure transducers have not yet been installed within the chambers and are currently positioned near the inlet channel for testing purposes. The electronics volume in this iteration has not been optimized, as the primary focus was on refining the mechanical structure. Future development will include designing a custom PCB to improve spatial efficiency and integration of the electronic components.

4.1 Design of the microgravity test rig
To validate IDRA, the inflatable chamber must be integrated with electric motors and rigid joints to construct the complete robotic system. In parallel with the development of the inflatable chambers, a robotic system with rigid links has been built to test control algorithms, including visual servoing techniques. This system is designed to easily replace the rigid links with the developed inflatable ones, which consist of multiple chambers. Subsequently, the robot must be tested in a microgravity facility to simulate space conditions. To achieve this, the project aims to develop a planar prototype of the robot.

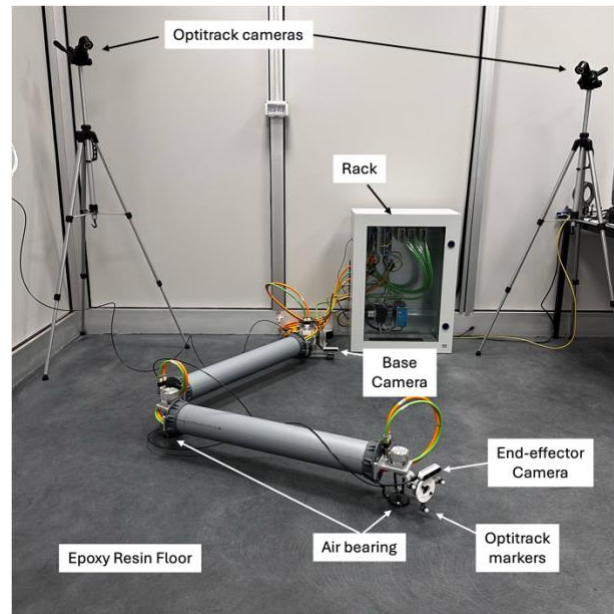In Fig 7, the robot with rigid links on the test bench for microgravity testing is shown.

Fig. 7. Robot for microgravity test on epoxy resin floor.

The test rig features an epoxy resin floor that provides a smooth surface, enabling air bearings to glide with minimal friction. The air bearings are attached to the robot at the locations of the electric motors, which are the heaviest components of the system. In the configuration shown, the cables must be replaced with lighter ones to

reduce their stiffness and minimize their impact on the robot's performance. A rack houses the drivers for the system. The robot's task is to reach a target using visual servoing techniques. Consequently, the robot is equipped with a camera mounted on its base to initially identify the target, and another camera is mounted on the end-effector for proximity operations to grasp the target. A grasping tool will be installed to perform this task. Finally, the test rig is equipped with an OptiTrack camera system, which allows for precise tracking of the robot's movements by using markers attached to the robot.

4. Testing

The objective of the test is to validate the chamber mechanism and the folding pattern, focusing on the retraction phase, which is the most critical. The tests are conducted using a prototype of the chamber that lacks the restraint layer, as they are performed at a low pressure of 12.5 kPa, eliminating the need for additional mechanical support. Furthermore, utilizing only the polyurethane layer facilitates inspection of the internal mechanism and the rigid ellipses during testing. The test bench is shown in Fig. 8. The test bench features a resin support that enables an air bearing to slide with minimal friction. One end of the chamber, referred to as the cap, is fixed, while the opposite end is free to move within a plane parallel to the resin support. A master board communicates with the Arduino Nano housed within the chamber, allow for the operations of the stepper motor. Rigid ellipses are mounted inside the bladder to create a folding pattern that enables controlled retraction while maintaining the cylindrical shape throughout the process.

The test starts by inflating the chamber, after which the outlet valve is activated for the duration of the test. Simultaneously, the stepper motor is engaged to pull the wire connected to the free cap. The mechanism previously shown in Fig. 6 is mounted on the fixed cap. The motion is captured by the OptiTrack camera following the installation of markers on the caps.
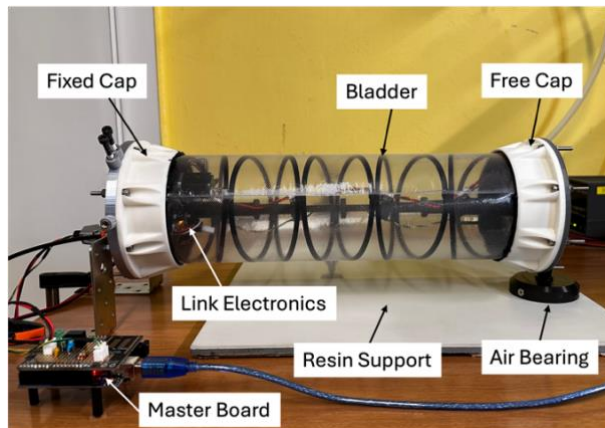

Fig. 8. Test bench for retraction tests of the inflatable chamber.

5. Results

The retraction test, illustrated in Fig. 9, demonstrates the transition from the inflated configuration (a) to the packed configuration (e).
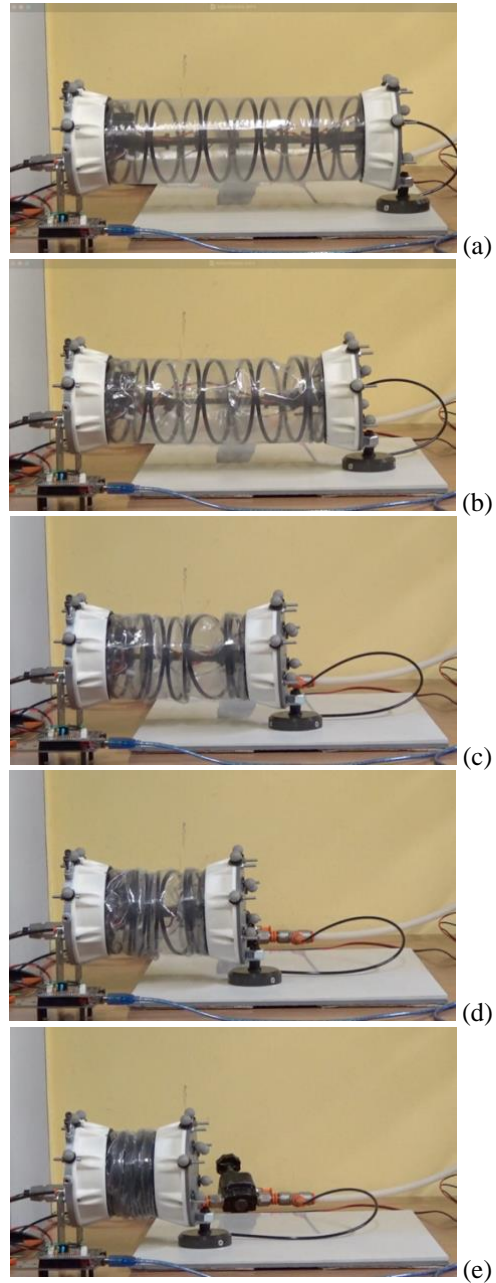

Fig. 9. Frames of the chamber retraction test: from inflated and deployed configuration (a) to packed configuration (e).

During this process, the free cap successfully slid along the resin support, and the stepper motor effectively pulled the free cap. The friction generated by the preliminary construction of the telescopic rod, produced using additive manufacturing techniques, was overcome

by the motor's force. The relative linear velocity between the free cap and the fixed cap was low, set at 2.3 mm/min. This reduced velocity facilitated efficient gas flow through the outlet valve, enhancing the overall performance of the chamber.

The OptiTrack data was analyzed to extrapolate the chamber length and angle deviation between caps throughout the test. Initially, when the chamber was fully inflated, corresponding to Fig. 9 (a), its length measured 405 mm. Upon activation of the outlet valve, the length decreased to 397 mm. Following the activation of the outlet valve, the stepper motor initiated its operation. In the packed configuration, corresponding to Fig. 9 (e), the length reached 143 mm. The chamber length is shown in Fig. 10 and angle deviation is shown in Fig.11.
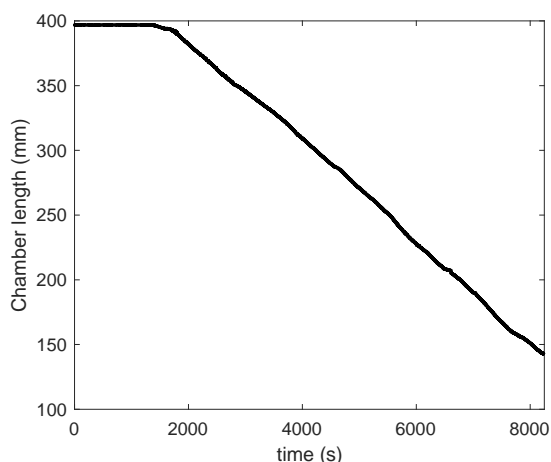

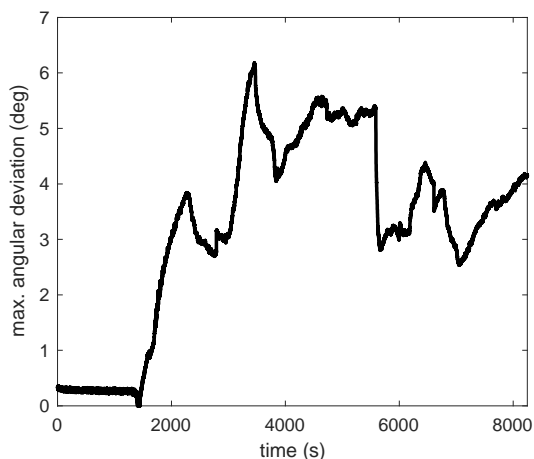Fig. 10. Chamber length during the retraction test, measured by the OptiTrack system.

Fig. 11. Maximum angular deviation between the caps during the retraction test, measured by the OptiTrack system.

Given that each cap represents a rigid, non-collapsible component with a length of 40 mm, the packing ratio of the chamber's soft section is approximately 5:1. This indicates that future prototypes should focus on minimizing the rigid components and optimizing the electronics. The results demonstrate a constant trend, with the free caps accurately following the motor's action at a constant velocity. However, some noise is introduced, visible analysing the maximum angle deviation during the test, due to friction within the telescopic rod, which requires further mitigation, and by the sequential packing of the elliptical structures that should be enhanced.

6. Conclusions

Following the introduction of IDRA, an inflatable robotic arm designed for space applications, this paper specifically focuses on the design of its inflatable links. The theoretical design process, material selection, layered structure, and the mechanism for controlled deployment and retraction are discussed. The latest developments in the design and construction of prototypes are presented, progressing from early prototypes fabricated using polymeric materials to the latest version, which incorporates a bladder layer, a restraint layer, and a controlled deployment and retraction mechanism. This design includes a folding pattern that enhances structural stability during both the deployment and retraction phases.

A dedicated facility for microgravity testing has been constructed to validate the performance of the robotic system. The test rig features an epoxy resin floor and air bearings designed to minimize friction and simulate microgravity conditions. Additionally, a planar version of the robot with rigid links has been developed to independently test control algorithms, including vision-based servoing techniques. The robot is designed to allow for the replacement of rigid links with inflatable ones once all validation tests have been successfully completed. This modular approach enables seamless integration of inflatable components following their performance verification.

A version of the link incorporating both a bladder and a deployment/retraction mechanism was tested in a retraction test, with measurements performed using the OptiTrack system. The results indicated that the chamber retracted at a constant velocity, as expected. However, some misalignments between the chamber's extremities were observed. These discrepancies could be attributed to the mechanical flexibility and friction of the telescopic rods, as well as the imperfect symmetry of the folding pattern. To address these issues, improvements in the fabrication process, particularly through refined additive manufacturing techniques, are necessary to reduce friction and enhance mechanical stability. Additionally, future design iterations will focus on optimizing the electronics and rigid caps of the chambers.

The next steps include conducting further tests on the retraction and deployment phases of the link, integrating the restraint layer, optimizing the electronics, installing

sensor transducers inside the chamber, and analyzing the wiring topology. Alternative folding patterns will also be evaluated. Once the inflatable chambers have been fully validated, tests in microgravity conditions will be conducted to assess the performance of the entire robotic system. Finally, the inflatable links will be tested the under extreme conditions, including high and low temperatures as well as vacuum environments.

Acknowledgements

References

[1] A. Flores-Abad, O. Ma, K. Pham, and S. Ulrich, "A review of space robotics technologies for on-orbit servicing," Prog. Aerosp. Sci., vol. 68, pp. 1–26, 2014, doi: 10.1016/j.paerosci.2014.03.002.

[2] On-Orbit Servicing, Assembly, and Manufacturing 2 (OSAM-2) https://www.nasa.gov/mission/on-orbit-servicing-assembly-and-manufacturing-2-osam-2/ [Online; Last Accessed: February, 2024]

[3] B. Ma, Z. Jiang, Y. Liu, and Z. Xie, "Advances in Space Robots for On-Orbit Servicing: A Comprehensive Review". Adv. Intell. Syst., 5: 2200397., 2023.

[4] https://space.skyrocket.de/doc_sdat/sentinel-1.htm

[5] Jameson, H., 2019. NSR Predicts Significant Growth Of In-Orbit Servicing Market Over Next Decade.

[6] ESPI, In-Orbit Services, Policy and Business Perspectives, 2020.

[7] NSR. 2020. In-Orbit Servicing: Technology and Market Readiness Undocked. [online] Available at: https://www.nsr.com/inorbit-servicing-technology-and-market-readiness-undocked/

[8] Global-On-Orbit-Satellite-Servicing-Market-Size: https://www.sphericalinsights.com/reports/on-orbit-satellite-servicing-market, last accessed: January 2024.

[9] NASA. On-orbit satellite servicing study project report. Technical Report, NASA; 2010

[10] A. Ellery, J. Kreisel, and B. Sommer, "The case for robotic on-orbit servicing of spacecraft: Spacecraft reliability is a myth," Acta Astronaut., vol. 63, no. 5–6, pp. 632–648, 2008.

[11] SatelliteXplorer https://geoxc-apps.bd.esri.com/ space/satellite-explorer/ [Online; Last Accessed: February, 2024]

[12] P. Anz-Meador, J. Opiela, and J.-C. Liou, "History of On-orbit Satellite Fragmentations, 16th Edition," no. December, 2022.

[13] Space In-Orbit Refueling Market Size, Share & Trends Analysis Report By Applications (Earth Observation, Communication, Navigation), By End-User (Commercial, Others), By Capability (Propellant Transfer, In-Orbit Rendezvous, In-Orbit Propellant Storage) and By Region(North America, Europe, APAC, Middle East and Africa, LATAM) Forecasts, 2021-2031

[14] A. Ogilvie, J. Allport, M. Hannah, and J. Lymer, "Autonomous robotic operations for on-orbit satellite servicing," Sensors Syst. Sp. Appl. II, vol. 6958, p. 695809, 2008, doi: 10.1117/12.784081.

[15] S. Jaekel et al., "Design and operational elements of the robotic subsystem for the e.deorbit debris removal mission," Front. Robot. AI, vol. 5, no. AUG, pp. 1–20, 2018, doi: 10.3389/frobt.2018.00100.

[16] https://www.spaceconomy360.it/missioni-spaziali/in-orbit-servicing-robotica-e-ai-per-allungare-la-vita-ai-satelliti/

[17] M. Pyrak and J. Anderson, "Performance of Northrop Grumman's Mission Extension Vehicle (MEV) RPO imagers at GEO," vol. 12115, p. 28, 2022, doi: 10.1117/12.2631524.

[18] S. V. Reznik, D. V. Reut, and M. S. Shustilova, "Comparison of geostationary and low-orbit 'round dance' satellite communication systems," IOP Conf. Ser. Mater. Sci. Eng., vol. 971, no. 5, 2020.

[19] M. Schenk, A. D. Viquerat, K. A. Seffen, and S. D. Guest, "Review of inflatable booms for deployable space structures: Packing and rigidization," J. Spacecr. Rockets, vol. 51, no. 3, pp. 762–778, 2014, doi: 10.2514/1.A32598.

[20] Y. Miyazaki and M. Uchiki, "Deployment Dynamics of Inflatable Tube," no. April, pp. 1–10, 2002.

[21] S. Sanan, J. B. Moidel, and C. G. Atkeson, "Robots with inflatable links," 2009 IEEE/RSJ Int. Conf. Intell. Robot. Syst. IROS 2009, pp. 4331–4336, 2009, doi: 10.1109/IROS.2009.5354151.

[22] J. M. A. Palacio, A. Riwan, N. Mechbal, E. Monteiro, and S. Voisembert, "A novel inflatable actuator for inflatable robotic arms," IEEE/ASME Int. Conf. Adv. Intell. Mechatronics, AIM, pp. 88–93, 2017, doi: 10.1109/AIM.2017.8014000.

[23] L. Salamina, D. Botto, S. Mauro, and S. Pastorelli, "Modeling of flexible bodies for the study of control in the simulink environment," Appl. Sci., vol. 10, no. 17, 2020, doi: 10.3390/app10175861.

[24] R. Freeland, G. Bilyeu, G. Veal, M. Steiner, and D. Carson, "Large inflatable deployable antenna flight experiment results," Acta Astronaut., 1998.

[25] H. de la Fuente, J. L. Raboin, G. R. Spexarth, and G. D. Valle, "TransHab: NASA's large-scale inflatable spacecraft," Collect. Tech. Pap. - AIAA/ASME/ASCE/AHS/ASC Struct. Struct. Dyn.

Mater. Conf., vol. 1, no. III, pp. 2157–2165, 2000, doi: 10.2514/6.2000-1822.

[26] Sierra Space. "Large Integrated Flexible Environment". sierraspace.com [On-line; Last Accessed: March, 2024].

[27] P. Laryssa, E. Lindsay, and O. Layi, "International space station robotics: a comparative study of ERA, JEMRMS and MSS," … Robot. …, pp. 1–8, 2002, [Online]. Available: http://robotics.estec.esa.int/ASTRA/Astra2002/Papers/astra2002_1.3-1.pdf.

[28] M. Bualat, J. Barlow, T. Fong, C. Provencher, T. Smith, and A. Zuniga, "Astrobee: Developing a free-flying robot for the international space station," AIAA Sp. 2015 Conf. Expo., pp. 1–10, 2015, doi: 10.2514/6.2015-4643.

[29] I. W. Park, T. Smith, H. Sanchez, S. W. Wong, P. Piacenza, and M. Ciocarlie, "Developing a 3-DOF compliant perching arm for a free-flying robot on the International Space Station," IEEE/ASME Int. Conf. Adv. Intell. Mechatronics, AIM, pp. 1135–1141, 2017, doi: 10.1109/AIM.2017.8014171.

[30] Palmieri, P., et al.: An Inflatable Robotic Assistant for Onboard Applications. In: Proceedings of the International Astronautical Congress, IAC, Dubai, United Arab Emirates, (2021).

[31] J. Hughes, U. Culha, F. Giardina, F. Guenther, A. Rosendo, and F. Iida, "Soft Manipulators and Grippers: A Review ," Frontiers in Robotics and AI , vol. 3. p. 69, 2016.

[32] L.S. Scimmi, M. Melchiorre, S. Mauro, and S. Pastorelli, "Experimental Real-Time Setup for Vision Driven Hand-Over with a Collaborative Robot". In: 2019 International Conference on Control, Automation and Diagnosis (ICCAD), Grenoble, France, 2019.

[33] P. Palmieri, et al. "Human Arm Motion Tracking by Kinect Sensor Using Kalman Filter for Collaborative Robotics". In: The International Conference of IFToMM ITALY, 2020.

[34] L.S. Scimmi, M. Melchiorre, M. Troise, S. Mauro, and S. Pastorelli, "A Practical and Effective Layout for a Safe Human-Robot Collaborative Assembly Task". Applied Sciences, 2021.

[35] M. Melchiorre, et al. "Robot Collision Avoidance based on Artificial Potential Field with Local Attractors." ICINCO. 2022

[36] M. Melchiorre, et al. "Experiments on the Artificial Potential Field with Local Attractors for Mobile Robot Navigation." Robotics 12.3 2023.

[37] Palmieri, P., Melchiorre, M., Mauro, S.: Design of a Lightweight and Deployable Soft Robotic Arm. Robotics, (2022).

[38] https://spacenews.com/41699italy-commits-more-funds-to-second-generation-radar-satellites/

[39] Palmieri, P. et al.: Inflatable Robotic Manipulator for Space Debris Mitigation by Visual Servoing, In: the 9th International Conference on Automation, Robotics and Application, (2023)

[40] Palmieri, P., Troise, M., Salamina, L., Gaidano, M., Melchiorre, M., Mauro, S. (2023). An Inflatable 7-DOF Space Robotic Arm for Active Debris Removal. In: Okada, M. (eds) Advances in Mechanism and Machine Science. IFToMM WC 2023. Mechanisms and Machine Science, vol 148. Springer, Cham.

[41] C. Wielgosz and J.C. Thomas. Deflections of inflatable fabric panels at high pressure. Thin-Walled Structures, 40(6):523–536, 2002.

[42] S. L. Veldman, O. K. Bergsma, and A. Beukers. Bending of anisotropic inflated cylindrical beams. Thin-Walled Structures, 43:461–475, 2005.

[43] I Weingarten, V, P. Seide, and J. P. Peterson. Buckling of Thin-Walled Circular Cylinders. NASA-SP-8007, 1968.

[44] G. D. Valle, D. Litteken, and T. C. Jones, "Review of Habitable Softgoods Inflatable Design, Analysis, Testing, and Potential Space Applications". In AIAA Scitech 2019 Forum, 2019.

[45] K. J. Kennedy, "ISS TransHab: Architecture Description". In International Conference On Environmental Systems. SAE International, 1999.

[46] J. Hinkle, A. Dixit, J. Lin, K. Whitley, J. Watson, and G. Valle, "Design development and testing for an expandable lunar habitat". Space 2008 Conference, 2008.

[47] L. Narici, M. Casolino, L. Di Fino, M. Larosa, P. Picozza, A. Rizzo, and V. Zaconte, "Performances of Kevlar and Polyethylene as radiation shielding on-board the International Space Station in high latitude radiation environment". Scientific Reports, 2017.

[48] M. Lambert, and E. Schneider, "Shielding against space debris. A comparison between different shields: The effect of materials on their performances". International Journal of Impact Engineering, 1995

[49] Mark Schenk, Andrew D. Viquerat, Keith A. Seffen, and Simon D. Guest. Review of inflatable booms for deployable space structures: Packing and rigidization. Journal of Spacecraft and Rockets, 51(3):762–778, 2014.

[50] Palmieri, P. et al.: A deployable and inflatable robotic arm concept for aerospace applications. In: 2021 IEEE 8th International Workshop on Metrology for AeroSpace, pp. 453-458, (2021).

[51] Y. Tago, Y. Satake and H. Ishii, "Novel Design of a Pneumatic Longitudinal Actuator for Both Extending and Contracting Motions," in IEEE Robotics and Automation Letters, vol. 9, no. 2, pp. 1436-1443, Feb. 2024